Supplementary Information

K^+ intercalated V_2O_5 nanorods with exposed facet as advanced cathodes for high energy and high rate zinc-ion batteries

Saiful Islam,[a‡] Muhammad Hilmy Alfaruqi,[ab‡] Dimas Y. Putro,[a] Vaiyapuri Soundharrajan,[a] Balaji Sambandam,[a] Jeonggeun Jo,[a] Sohyun Park,[a] Seulgi Lee,[a] Vinod Mathew,[a] Jaekook Kim[a*]

[a]Department of Materials Science and Engineering, Chonnam National University, 300 Yongbong-dong, Buk-gu, Gwangju 61186, Republic of Korea

[b]Departemen Teknik Metalurgi, Universitas Teknologi Sumbawa, Jl. Raya Olat Maras, Sumbawa, Nusa Tenggara Barat 84371, Indonesia

‡ These authors contributed equally to this work.
* Corresponding author. Tel: +82-62-530-1703. Fax: +82-62-530-1699.
E-mail: jaekook@chonnam.ac.kr (Jaekook Kim)

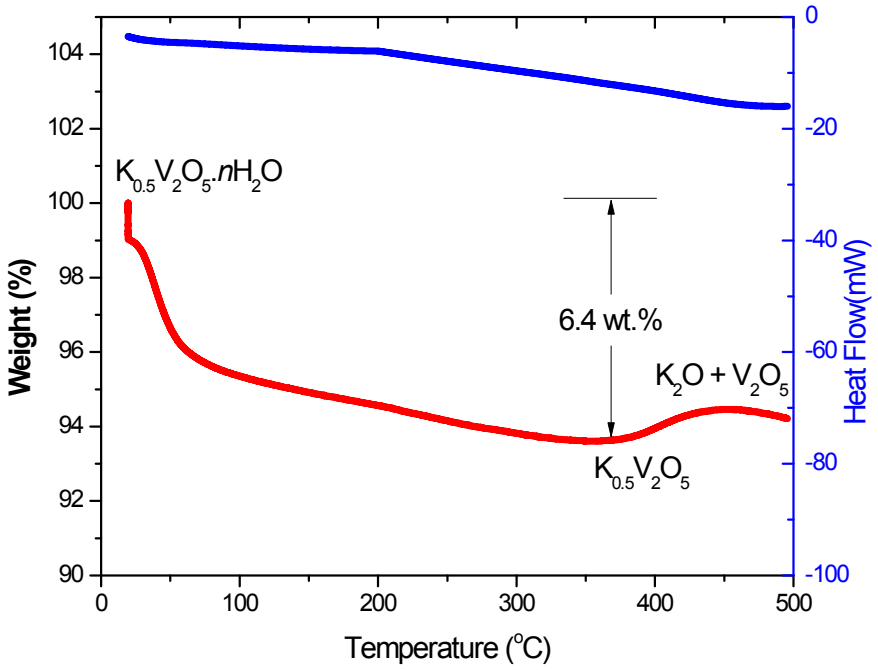

Fig. S1 TGA curve of the KVO powder. Weight decreased up to 350 ˚C and the increased because of the oxidation of metal. Further, at elevated temperature, it may decompose into K_2O and V_2O_5.

Table S1 Crystallographic data of the KVO powder obtained from Rietveld refinement.

R_p = 18.07, R_{wp} = 18.45, R_{exp} = 15.87, GoF = 1.35						
KVO	a = 3.66318, b = 11.5989, c = 18.7587, α = 90°, β = 90°, γ = 90°					
	Atom	**Site**	**Wyckoff positions**			**Occupancy**
	V	8*f*	0	0.06574	0.0791	1
	V	8*f*	0	0.23111	0.57982	1
	K	4*c*	0	0.42	0.25	0.5
	O	8*f*	0	0.081	0.547	1
	O	8*f*	0	0.0481	0.1645	1
	O	8*f*	0	0.2121	0.6649	1
	O	8*f*	0	0.2411	0.05779	1
	O	8*f*	0	0.6011	0.06511	1
	O	4*c*	0	0.2	0.25	0.76
	H	8*f*	0	0.165	0.295	0.76

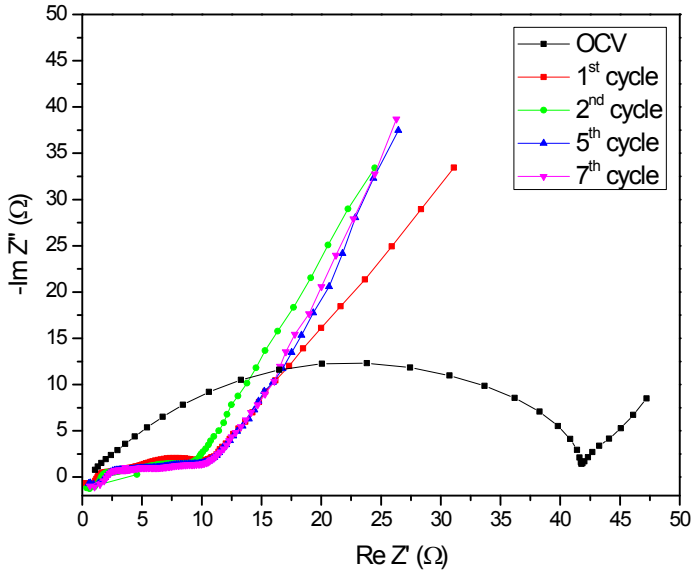

Fig. S2 Comparison of electrochemical impedance spectra of Zn/KVO cells at OCV and after the 1st, 2nd, 5th and 7th cycles.

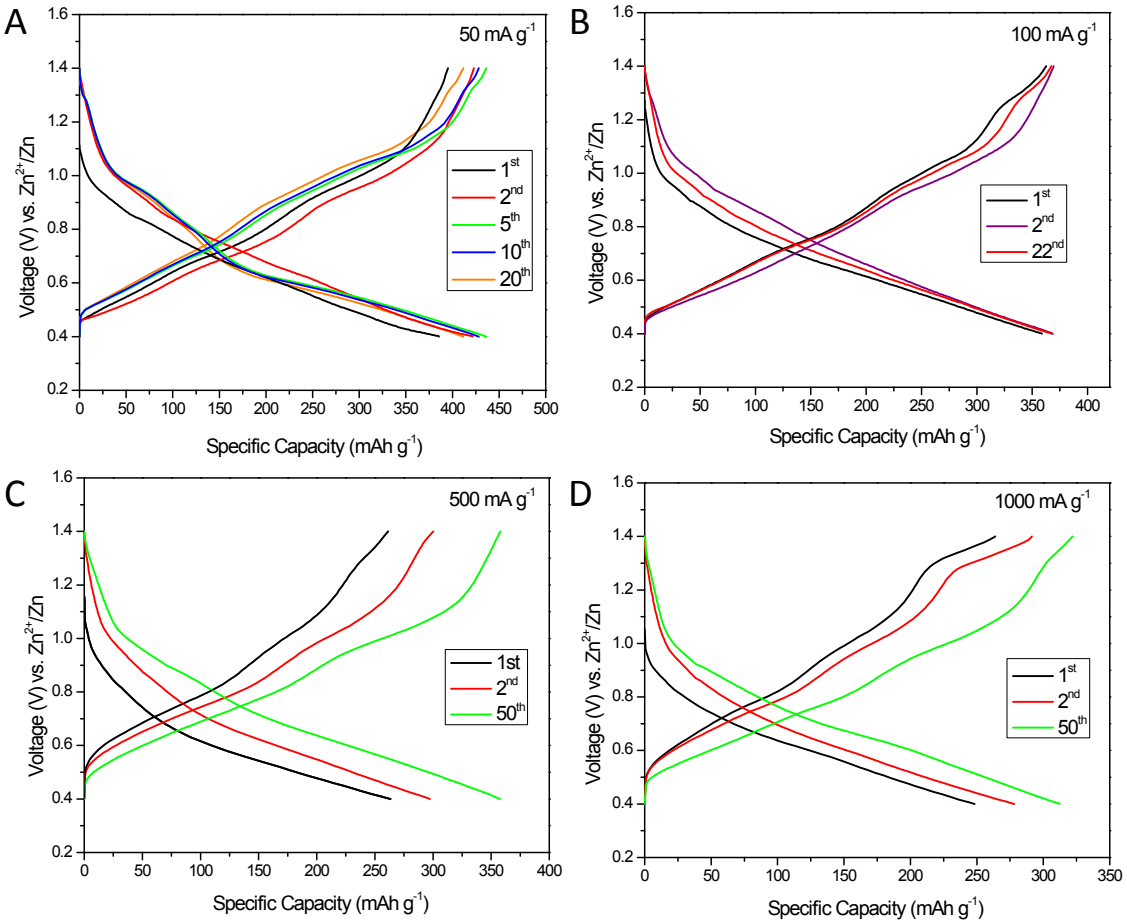

Fig. S3 Charge/discharge profiles of the KVO cathode at various rates. (A) 50, (B) 100, (C) 500 and (D) 1000 mA g^{-1}.

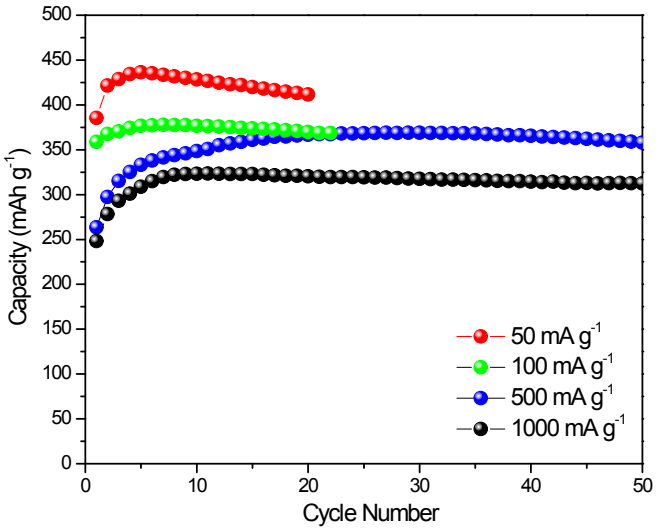

Fig. S4 Cycleability data of the KVO cathode at 50, 100, 500 and 1000 mA g^{-1}.

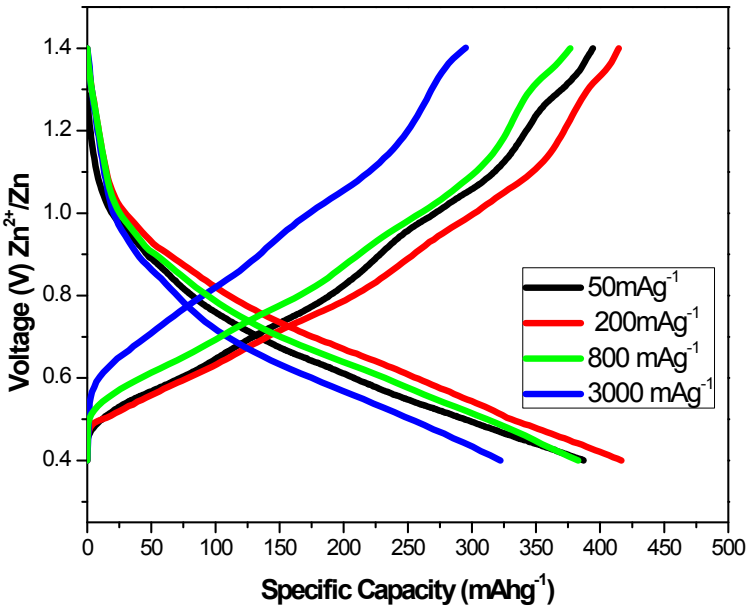

Fig. S5 Discharge/charges profile of KVO at different current rates within the potential window of 0.4 to 1.4 V.

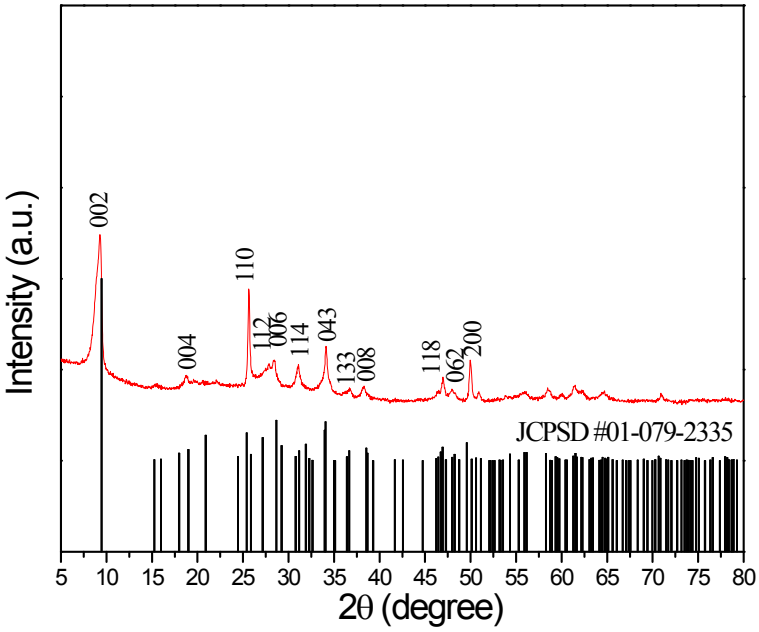

Fig. S6 XRD pattern of the KVO-C sample.

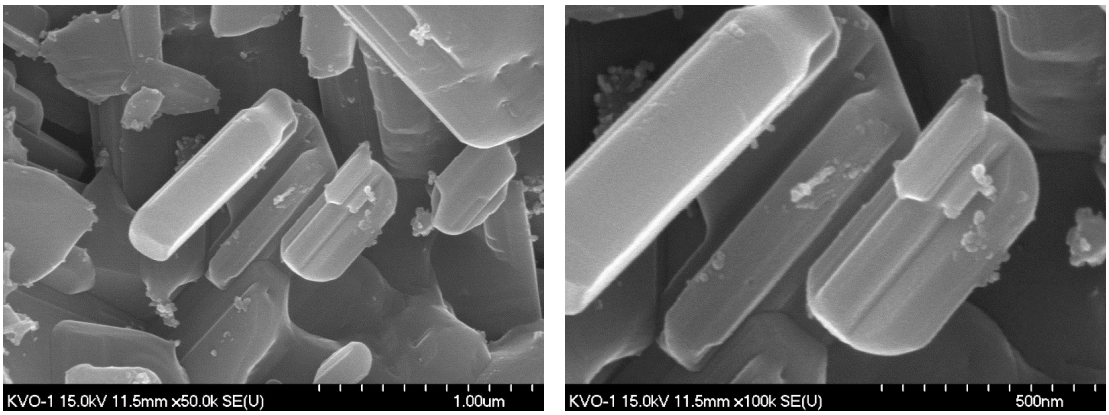

Fig. S7 SEM images of the KVO-C sample.

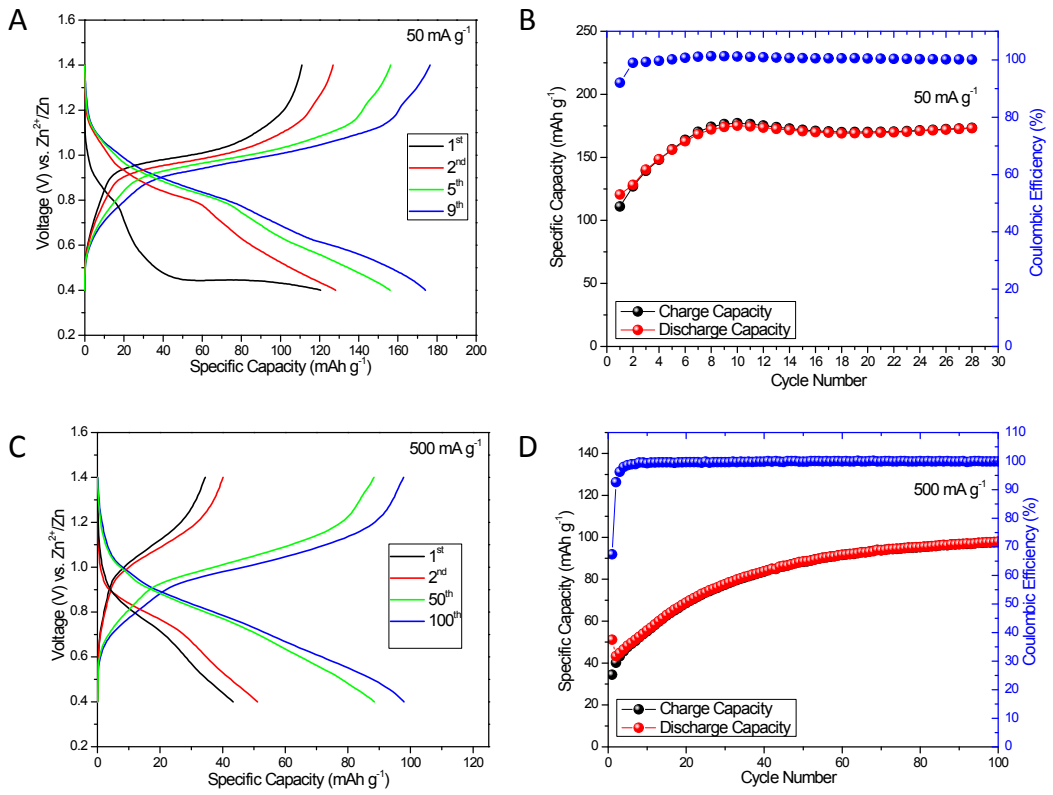

Fig. S8 Electrochemical performance of the KVO-C cathode in Zn test cell. Charge/discharge profiles at (A) 50 and (C) 500 mAh g^{-1}. Cycleability data at (B) 50 and (D) 500 mAh g^{-1}.

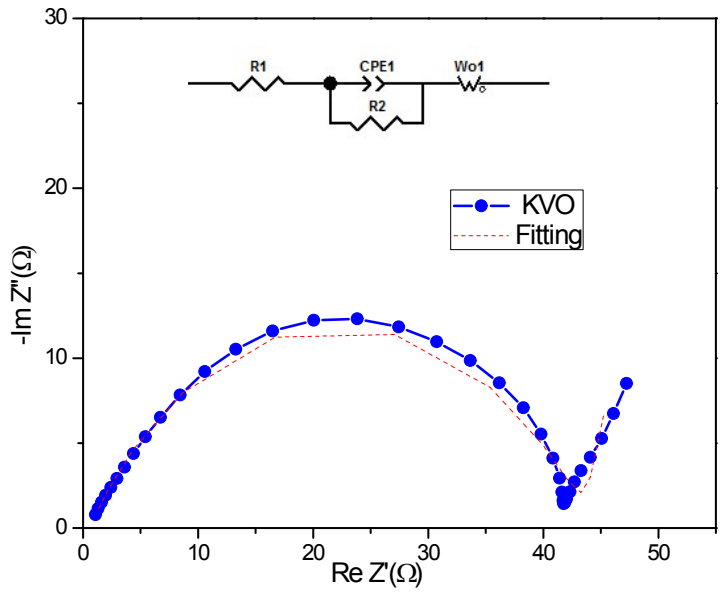

Fig. S9 Nyquist plot for as prepared Zn/KVO cell with its corresponding equivalent circuit.

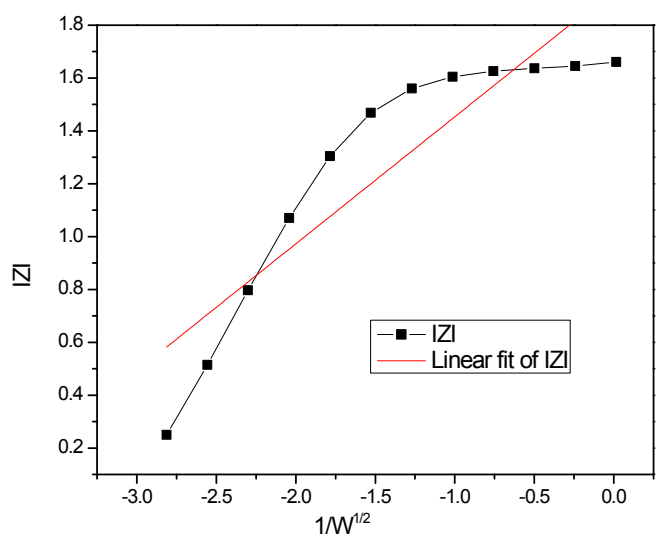

Fig. S10 Linear fitting to Impedance ([Z]) *vs.* radial frequency (w) curve for impedance analysis.

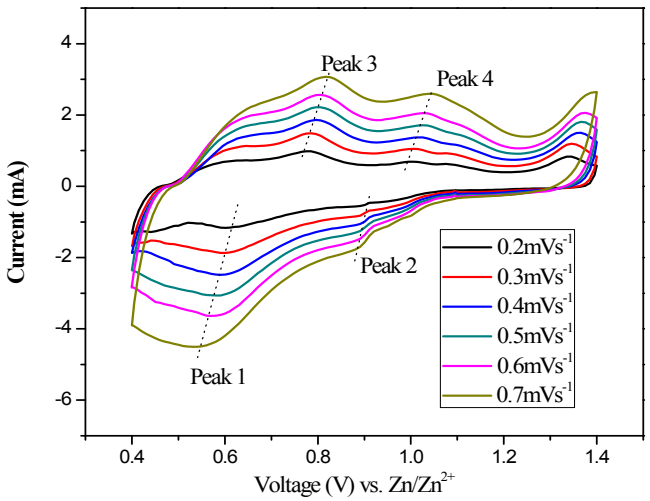

Fig. S11 CV curves of Zn/KVO cells at different scan rate.

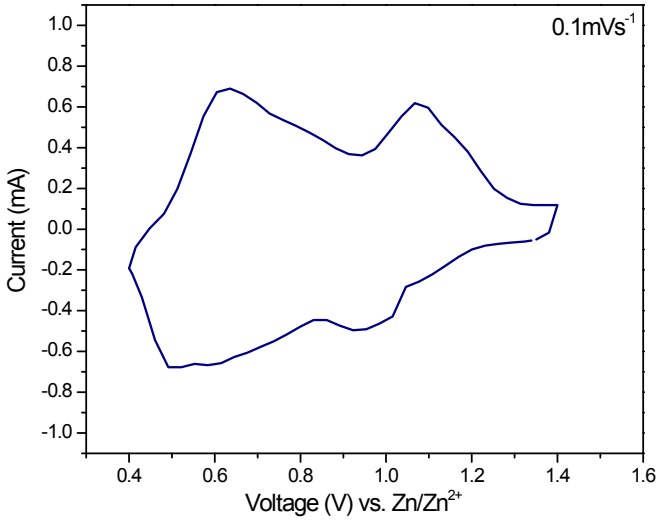

Fig. S12 CV plot of the KVO electrode at a scan rate of 0.1 mV s^{-1}.

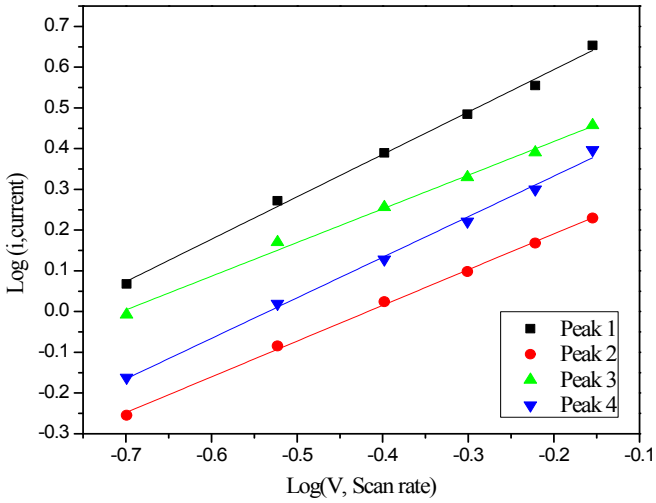

Fig. S13 Log(*i*) *vs.* log(*v*) plots at specific peak currents.

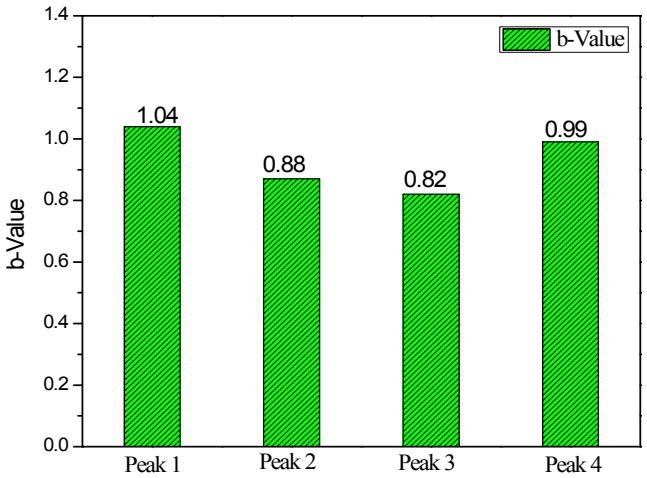

Fig. S14 The *b*-values calculated at different redox peaks.

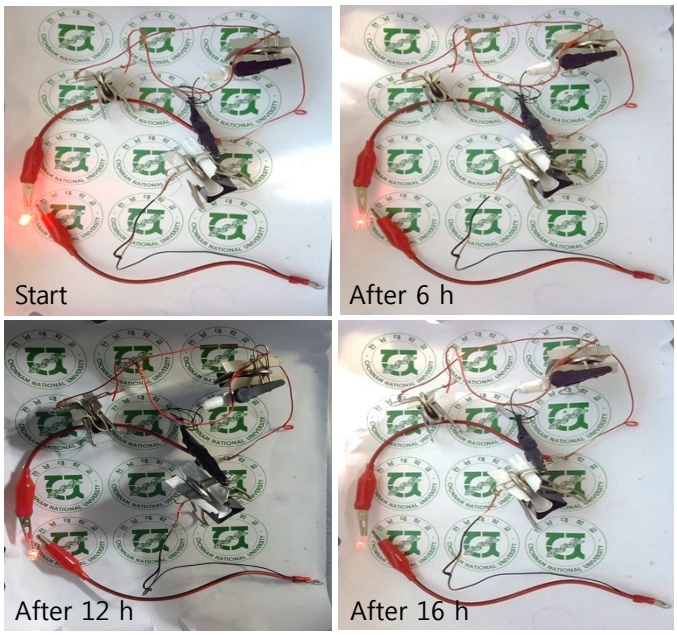

Fig. S15 Digital image of Zn/KVO battery to power an external red LED.

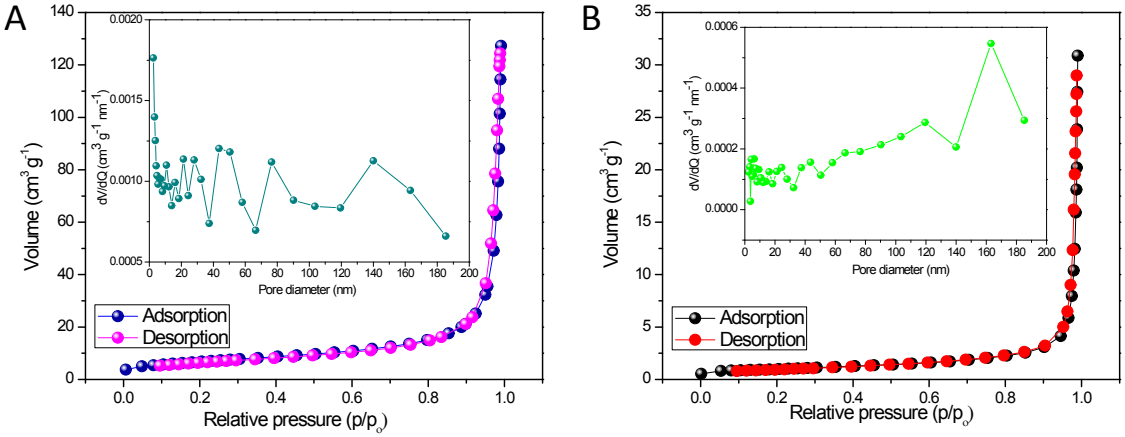

Fig. S16 N_2 absorption/desorption isotherm and pore size distribution plots of the (A) KVO and (B) V_2O_5 electrodes.

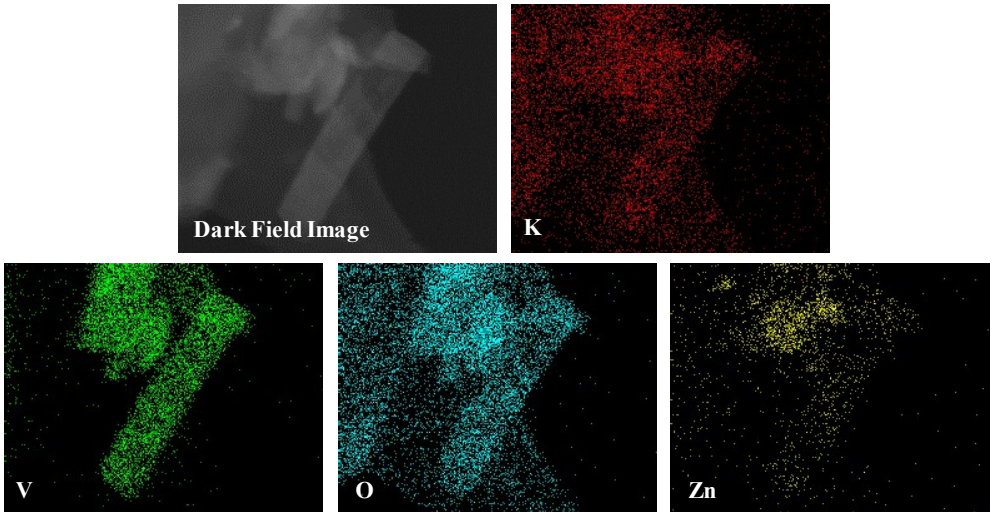

Fig. S17 *Ex situ* EDX elemental mapping of the discharge KVO electrode.

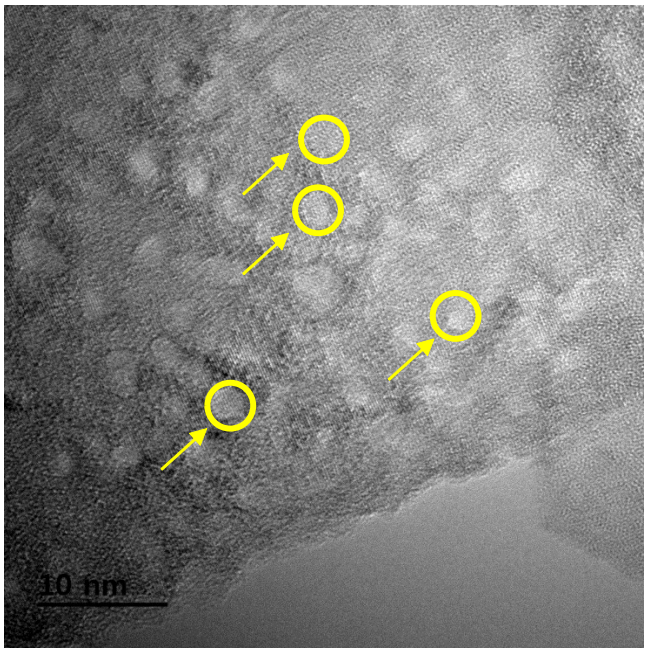

Fig. S18 *Ex situ* TEM image of the discharged KVO electrode. It can be seen that the spherical particle of phase was attached on the electrode surface.

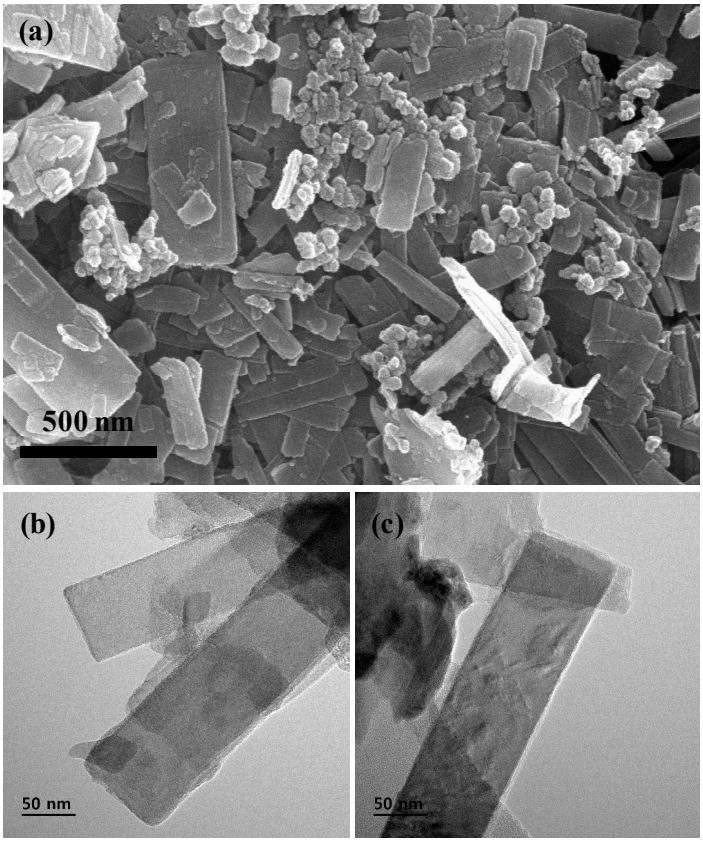

Fig. S19 *Ex situ* (a) SEM and (b,c) TEM images of the discharge KVO electrodes.

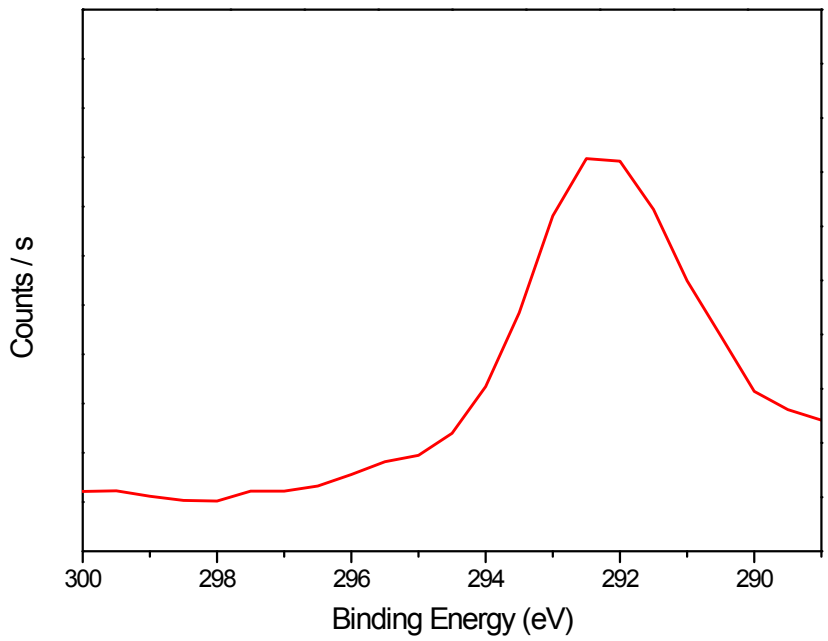

Fig. S20 *Ex situ* XPS spectrum of K element after cycling.

Table S2 *Ex situ* ICP measurements of electrolytes after cycling.

Sample	**Element**	**Wavelength (nm)**	**Concentration (ppm)**
KVO-1D	K	766.49	0.33
KVO-1C	K	766.49	0.27

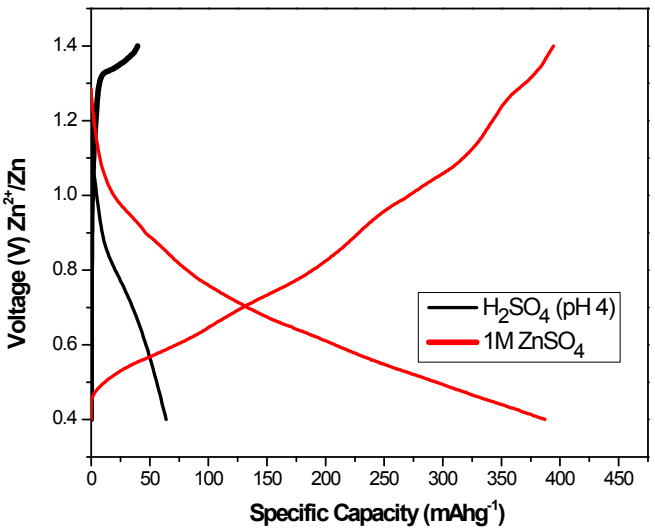

Fig. S21 Electrochemical charge/discharge of the KVO electrolyte using dilute H_2SO_4 (pH 4) and 1 M $ZnSO_4$ electrolytes.

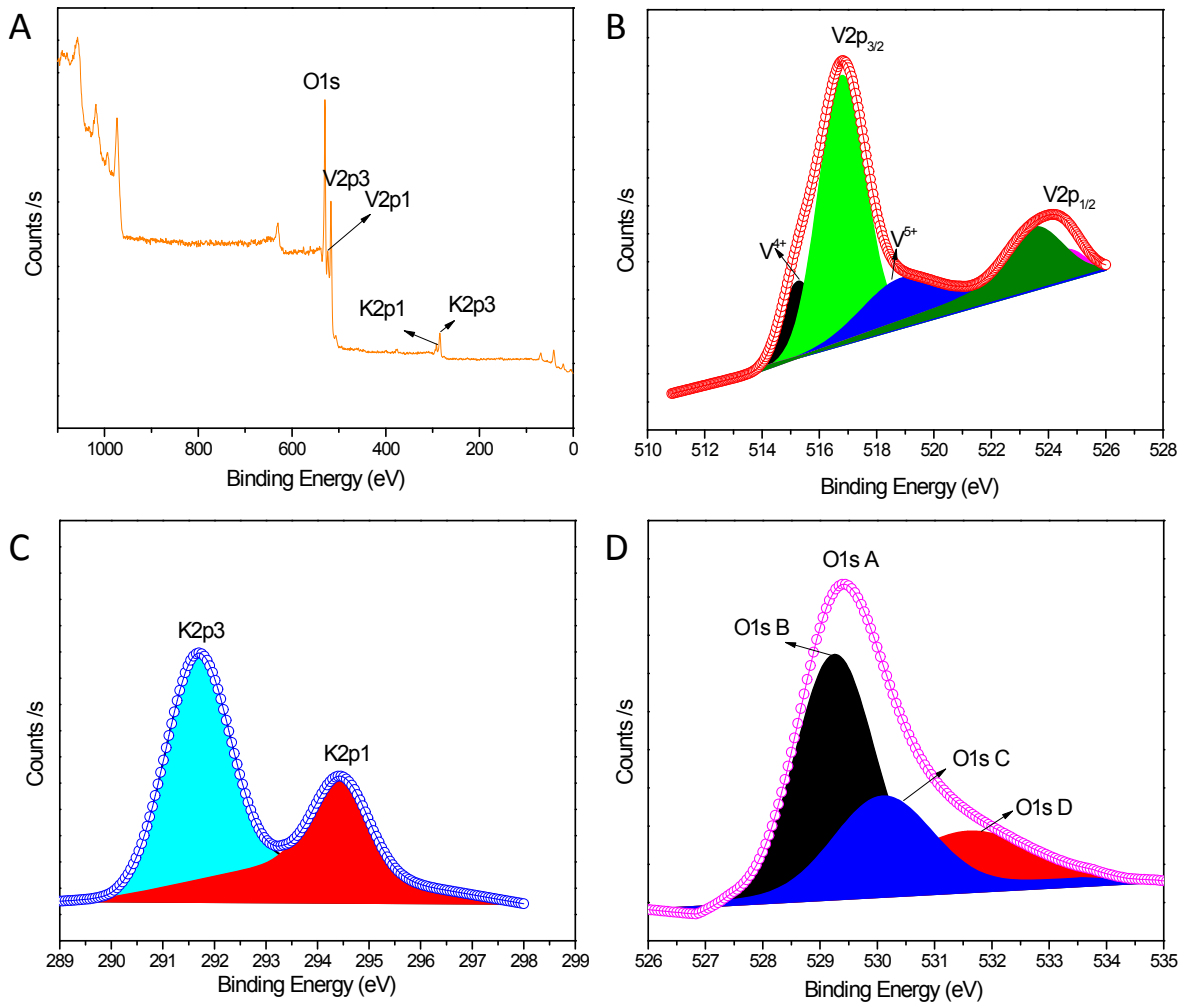

Fig. S22 XPS (A) survey, (B) V, (C), K and (D) O spectra of the KVO sample.

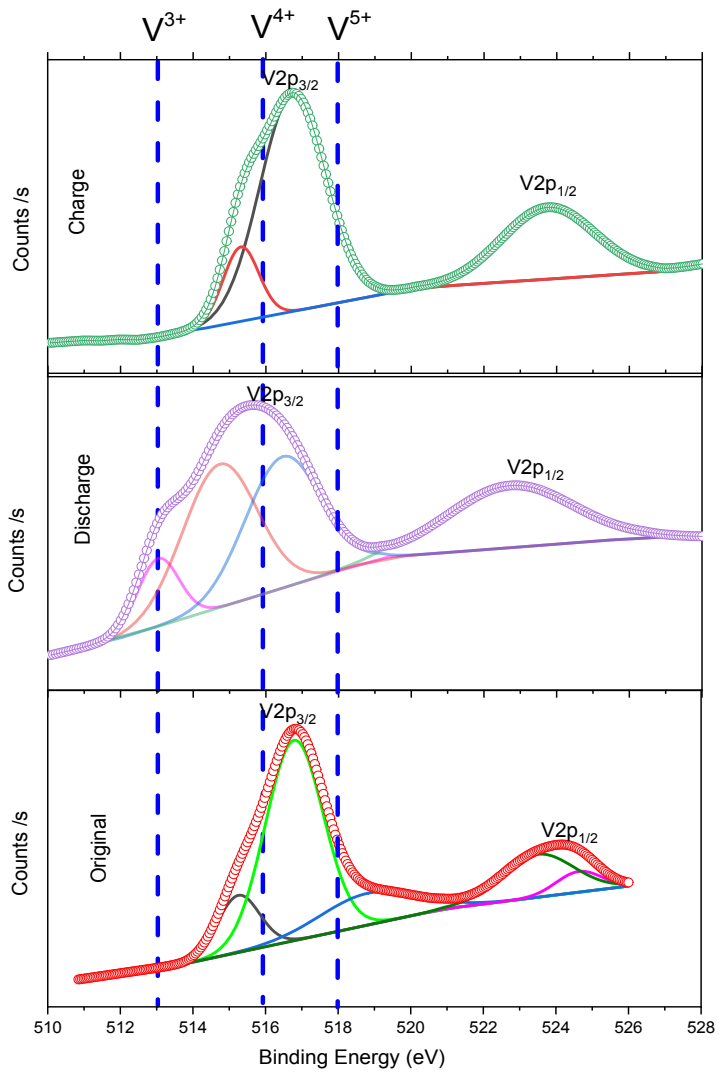

Fig. S23 *Ex situ* XPS spectra of the KVO electrode before electrochemical reaction, after discharging and after charging.

Table S3 Calculated lattice parameters of KVO obtained from experimental and DFT calculations.

$K_{0.5}V_2O_5$	*a*	*b*	*c*	α,β,γ (deg)
Rietveld	3.66318	11.5989	18.7587	90
DFT	3.62891	11.30894	17.99323	90

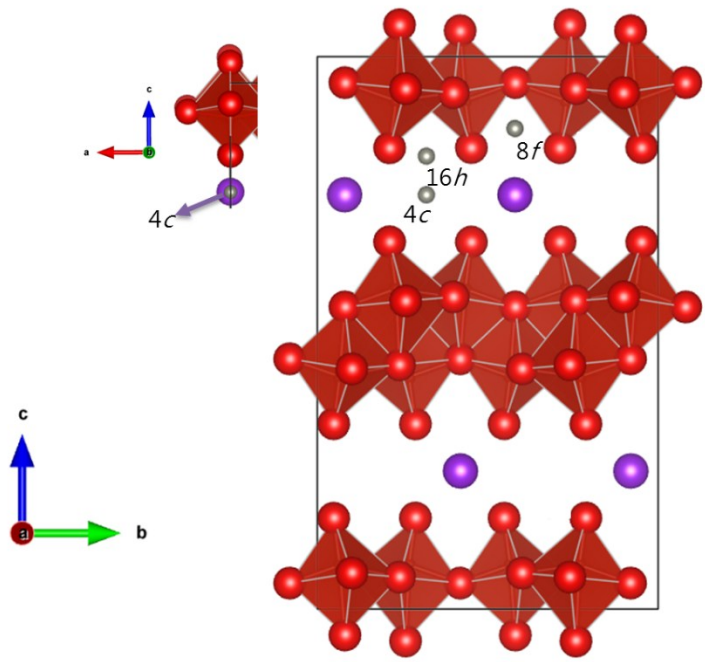

Fig. S24 Possible Zn locations in the KVO structure.

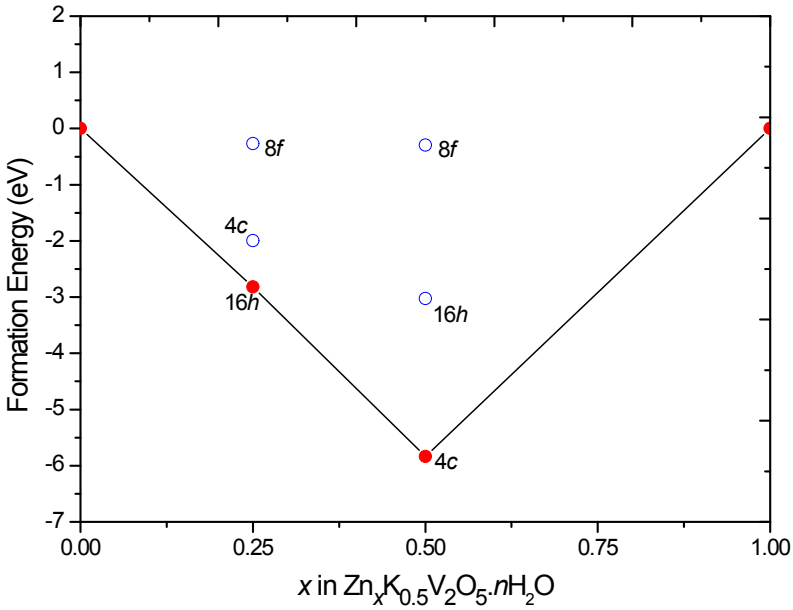

Fig. S25 Convex hull and the formation energy of the Zn-intercalated KVO systems.

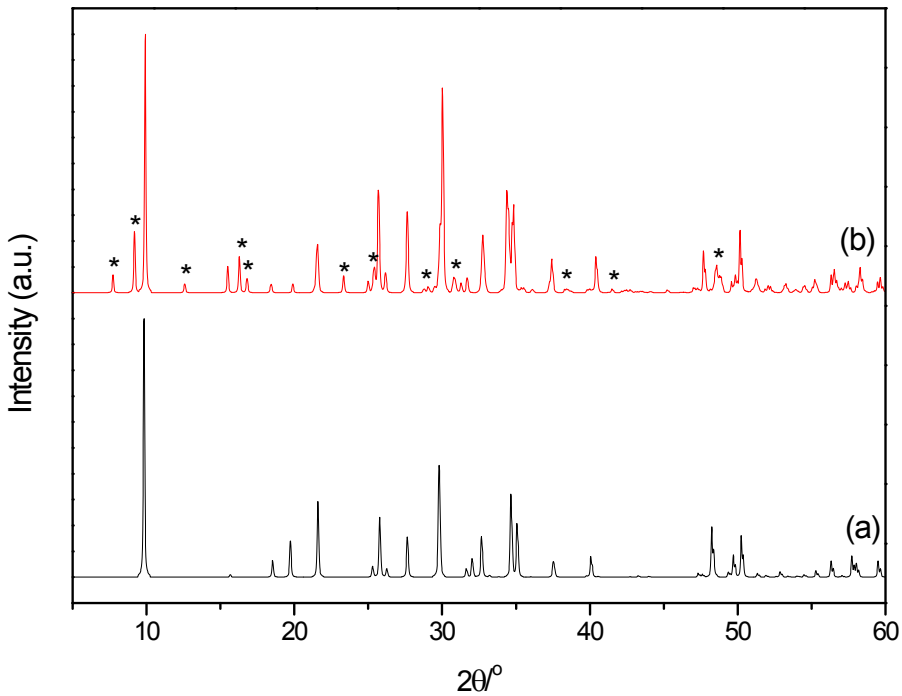

Fig. S26 Simulated XRD patterns of the (a) KVO and (b) Zn-inserted KVO structures obtained from DFT calculations.

ESI Note 1

The theoretical capacity (Q) can be estimated using the Faraday equation:

$$Q = \frac{n \times F \times 1000}{Mw \times 3600},$$

where *n* is the number of electron involved, *F* is the Faraday's constant and *Mw* is the dehydrated molecular weight. Suppose the *n* value is 3.5, in which the V is completely reduced to V(III) state (close to the XAS and XPS measurements); and hence, the Q could be then calculated to be 465 mAh g^{-1}. Note that the capacitive reaction may also contribute to the capacity, as observed from CV measurements. This also in agreement with the previous reports.[SI1-SI3]

ESI Note 2

The KVO-C was prepared using solvent dry synthesis. In brief, stoichiometric amount of KOH and V_2O_5 were dissolved in DI water and stirred overnight. The stirred solution was then dried at 80 ˚C before annealing at 400 ˚C for 4 h.

References

[SI1] N. Zhang, Y. Dong, M. Jia, X. Bian, Y. Wang, M. Qiu, J. Xu, Y. Liu, L. Jiao, F. Cheng, *ACS Energy Lett.*, 2018, 3, 1366.

[SI2] C. Xia, J. Guo, P. Li, X. Zhang, H.N. Alshareef, *Angew. Chem. Int. Ed.*, 2018, 57, 3943.